ACS chemical biology

Letters

pubs.acs.org/acschemicalbiology

Visualizing the 16-Membered Ring Macrolides Tildipirosin and Tilmicosin Bound to Their Ribosomal Site

Jacob Poehlsgaard,[†,§] Niels M. Andersen,[†] Ralf Warrass,[‡] and Stephen Douthwaite*[,†]

[†]Department of Biochemistry & Molecular Biology, University of Southern Denmark, Campusvej 55, DK-5230 Odense M, Denmark

[‡]MSD Animal Health Group, Intervet Innovation GmbH, Zur Propstei, D-55270 Schwabenheim, Germany

Supporting Information

ABSTRACT: The veterinary antibiotic tildipirosin (20,23-dipiperidinyl-mycaminosyl-tylonolide, Zuprevo) was developed recently to treat bovine and swine respiratory tract infections caused by bacterial pathogens such as *Pasteurella multocida*. Tildipirosin is a derivative of the naturally occurring compound tylosin. Here, we define drug–target interactions by combining chemical footprinting with structure modeling and show that tildipirosin, tylosin, and an earlier tylosin derivative, tilmicosin (20-dimethylpiperidinyl-mycaminosyl-tylonolide, Micotil), bind to the same macrolide site within the large subunit of *P. multocida* and *Escherichia coli* ribosomes. The drugs nevertheless differ in how they occupy this site. Interactions of the two piperidine components, which are unique to tildipirosin, distinguish this drug from tylosin and tilmicosin. The 23-piperidine of tildipirosin contacts ribosomal residues on the tunnel wall while its 20-piperidine is oriented into the tunnel lumen and is positioned to interfere with the growing nascent peptide.

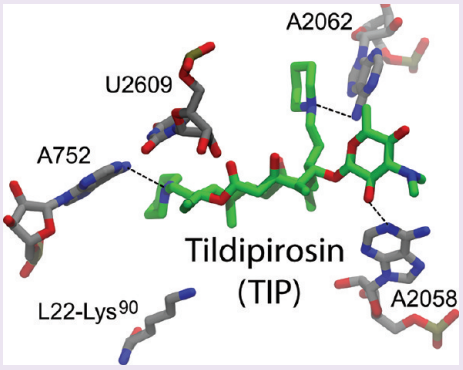

Tildipirosin (TIP) has recently been approved in Europe to treat bovine and swine respiratory tract infections and is structurally similar to tilmicosin (TIL); both of these drugs are derived from the naturally occurring 16-membered ring macrolide tylosin (TYL, Figure 1). TYL and most other macrolides are not generally indicated for use against Gram-negative pathogens due to their limited capacity to penetrate the outer membrane of these bacteria. TIP, on the other hand, shows much better membrane penetration presumably due its two piperidine rings that contribute both hydrophobic and basic properties (Figure 1) and is thus effective against Gram-negative pathogens including *Mannheimia haemolytica* and *Pasteurella multocida*,[1] which are the two main etiological agents of bovine respiratory tract infections.[2]

The need for new antimicrobials to combat such pathogens has recently been underlined by reports of resistance not only to macrolides but also to aminocyclitols, amphenicols, β-lactams, fluoroquinolones, sulfonamides, and tetracyclines in strains of *M. hemolytica* and *P. multocida*.[3,4] The mechanisms of macrolide resistance in these strains have recently been shown to involve *msr(E)*-encoded drug efflux, *mph(E)*-encoded drug phosphorylation, and *erm(42)*-encoded rRNA methylation.[5−7] Some highly resistant strains possess all three of these determinants, while other less resistant strains rely on one or two of the mechanisms. For instance, one subset of resistant strains lacks the *erm(42)* gene but possesses the tandemly coupled *msr(E)* and *mph(E)* genes.[6] The resistance mechanisms encoded by *msr(E)* and *mph(E)* show little to no activity against 16-membered macrolides, and thus TIP remains effective against strains harboring these determinants.

In addition to the ability to penetrate bacterial membranes and side-step resistance mechanisms, other important pharmacodynamic properties of antimicrobial compounds are defined by their interactions at the inhibitory target. The target site interactions of TYL have been studied in molecular detail by crystallographic,[8,9] biochemical,[10,11] and genetic approaches,[12] and this contrasts with the lack of available structural information for the more commonly used, newer derivatives TIL and TIP. Here, we define the target site of these macrolides on *P. multocida* and *Escherichia coli* ribosomes by chemical footprinting and combine these data with molecular modeling to determine the orientations and contacts of the drugs within their ribosomal site. Novel interactions made by the dimethylpiperidine and piperidine substituents in TIL and TIP explain their mode of action and provide a basis for further drug development by rational design.

Chemical Footprinting of Macrolides Bound to Their Ribosomal Site. The footprint data showed that the macrolide drugs interact in essentially the same manner to both the *E. coli* and *P. multocida* ribosomes (Figure 2), reflecting the high degree of conservation of the drug binding site in these two bacteria. The macrolides bind within the tunnel of the 50S ribosomal subunit and make several common contacts with 23S rRNA nucleotides. Similarities in the drug–rRNA interactions would be expected given the common structural features, including the 16-membered tylonolide ring and mycaminose

Received: March 7, 2012
Accepted: May 7, 2012
Published: May 7, 2012

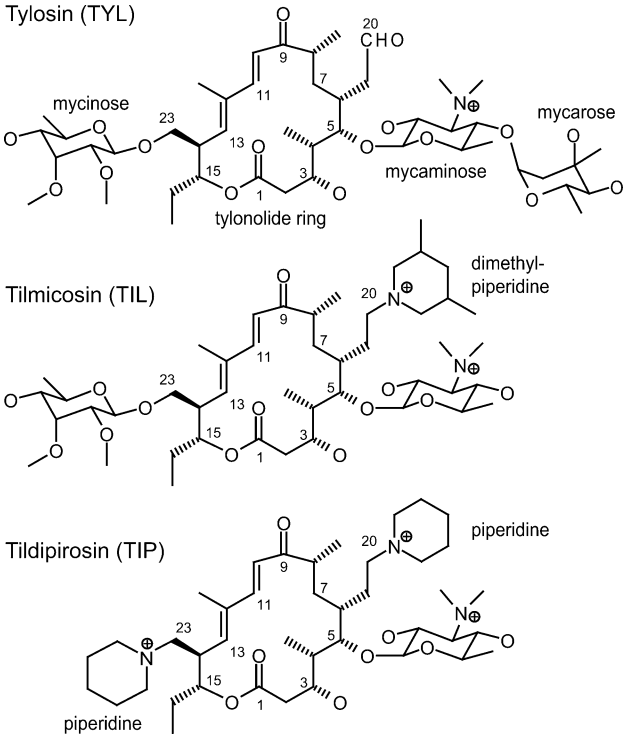

Figure 1. Chemical structures of the 16-membered ring macrolides used in the study. Tilmicosin (TIL) and tildipirosin (TIP) are derivatives of tylosin (TYL) and have retained the 16-membered macrolactone (tylonolide) ring and the 5-mycaminose amino sugar. The drugs are distinguished by the mycarose sugar in TYL, the 20-dimethylpiperidine in TIL, and the 20- and 23-piperidines in TIP. The different substituents result in one, two, and three basic centers (+) in TYL, TIL, and TIP, respectively.

sugar that TIP and TIL share with TYL (Figure 1), which play major roles in ribosome interaction.[8,13] Looking beyond these similarities, however, the data revealed subtle differences in the patterns of drug−rRNA contact (Table 1) that would influence both drug interaction and affinity for the target.

The main drug interactions are with nucleotides A2058 and A2059, while other tunnel nucleotides are also in close proximity as seen in previous studies for TYL.[10,11] Protection at U2609 from CMCT modification was common to all the macrolides, whereas only TYL protected at U2506 through its mycarose moiety,[10] which is absent in TIP and TIL (Figure 1). Other differences between TYL and its derivatives were seen in the accessibility at nucleotide A2062 (Figure 2a). In the crystal structure, the N6 position of A2062 forms a covalent bond with the 20-aldehyde group of TYL,[8] and this interaction is important for drug binding and inhibition (refs 9 and 14 and references therein). The loss of the covalent bond can, however, be compensated by hydrophobic aminoalkyl modifications at the 20-position that have been proposed to stack onto the A2062 base.[14] The footprinting data show how TYL protects A2062 from modification by DMS, while the 20-piperidine and dimethylpiperidine groups of TIP or TIL preclude any covalent interaction and enhance the accessibility of A2062 to the DMS probe (Figure 2a). On the other side of the ribosome tunnel, the reactivity at A752 was reduced by TYL and TIL, whereas TIP, which lacks the 23-mycinose sugar, slightly enhanced the accessibility of A752 (Figure 2b and Table 1). These data were used as a basis for molecular modeling to determine the orientation of the drugs within the ribosomal tunnel and the contacts made with the rRNA.

Macrolide−Ribosome Modeling System. The modeling system was based on the *E. coli* ribosome structure[15] and limited in size to include ribosomal residues that had at least one atom within 15 Å of the macrolide binding site. The system was subjected to conformational searches in the absence of macrolides to find possible orientations of the binding site nucleotides. Similarly, conformational searches were performed on unbound TYL, TIP, and TIL molecules to determine their lowest energy structures. In free solution, the additional piperidine and dimethylpiperidine groups did not appreciably change the conformation of the tylonolide ring in TIP and TIL relative to TYL (Supplementary Figure 1a).

When placed into the modeling system, TYL engaged in the same hydrogen bonding interactions with 23S rRNA that were previously proposed for the *Haloarcula marismortui* ribosome.[8] Steric clashes were minimal, and the only major overlap requiring readjustment was between TYL and Lys90 of r-protein L22 (Supplementary Figure 1). The validity of the computational approach was tested by superimposing the modeled and crystal structures of TYL (Supplementary Figure 2), where the two structures were seen to be highly similar with a heavy atom root-mean-square deviation of 0.9 Å.

Modeling TIL and TIP on the Ribosome. The free-solution structures of TIL and TIP were superimposed onto TYL in each of the five lowest energy conformations for the ribosome model. The resultant complexes retained the A2058−mycaminose interaction seen for TYL (Supplementary Figure 1). A different interaction was required at A2062, where only one of the conformations of this nucleotide avoided a clash with the drugs. This conformation was subjected to constrained minimization and revealed a new putative electrostatic interaction between the N6 position of A2062 and the nitrogen of the TIP 20-piperidine (or the TIL 20-dimethylpiperidine). For both drugs, this interaction required a shift from sp2 to sp3 hybridization of the N6 amine of A2062. Further analyses by quantum mechanics showed that the energy change for the optimal complex was approximately −30 kJ mol^{-1} and included charge electrostatic and dispersion interactions between the π orbitals of the adenine and the sp3 orbitals of the 20-piperidine/20-dimethylpiperidine (Supplementary Figure 3). In addition to hydrogen bonding with the N6 of A2062, van der Waals interactions between the adenine base and the 20-substituents of TIP and TIL (Supplementary Figure 1c and 1d) would contribute an appreciable portion of the total drug binding energy. The conformation of A2062 would be altered in different ways by the TYL bond and the TIP/TIL interactions, and changes in the orientation of this nucleotide within the ribosomal tunnel have been previously been linked to stalling of protein synthesis (ref 16 and references therein). It is thus noteworthy that the accessibility of A2062 to chemical probes is altered by macrolides[10,17] and ketolides[18,19] that are potent inhibitors of protein synthesis.

At the other side of the drug binding site, TIL retained the A752−mycinose interaction seen for TYL (Supplementary Figures 1 and 4). The corresponding position of the TIP structure lacks the mycinose sugar and is substituted with the 23-piperidine, which was shown by chemical footprinting (Table 1) to interact in a different manner with the ribosome tunnel (Figure 3). The exact orientation of the 23-piperidine would depend on its protonation state. The pK_a values of the three basic centers in TIP were measured at 8.1 for the mycaminose nitrogen and at 8.8 and 9.9 for the two piperidine

dx.doi.org/10.1021/cb300105p | *ACS Chem. Biol.* 2012, 7, 1351−1355

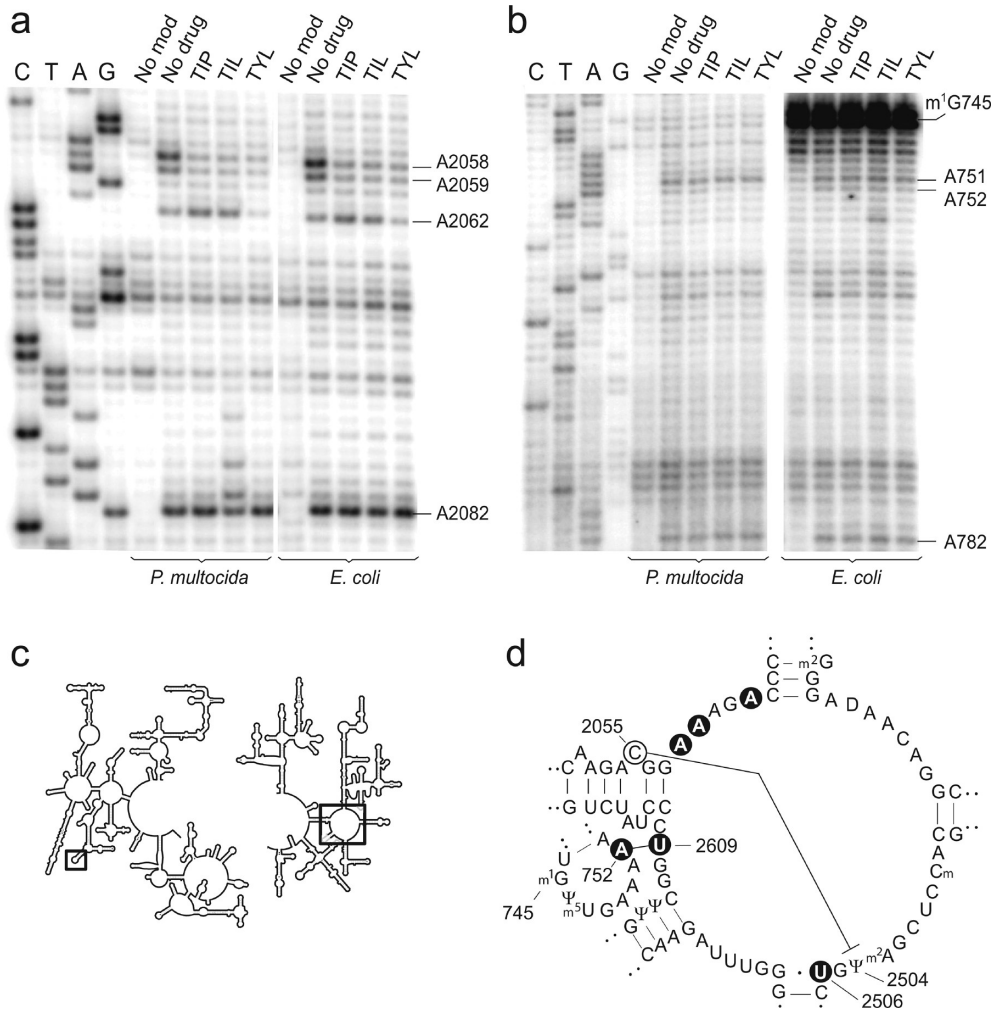

Figure 2. Interactions of the macrolides on rRNA. (a) Drug binding effects in the 2058 region of 23S rRNA on ribosomes from *P. multocida* and *E. coli*. Control samples were without modification (No mod) or DMS modified without any drug bound (No drug); the macrolides tildipirosin (TIP), tilmicosin (TIL), and tylosin (TYL) were present at 20 μM. (b) DMS footprinting in the 750 region of 23S rRNA. The *E. coli* 23S rRNA has an m^1G745 modification evident as a strong stop band; there is no such modification in the *P. multocida* rRNA. (c) Structure of bacterial 23S rRNA indicating the positions of the 750 and 2058 regions (boxes). (d) Enlargement of the boxed structures showing how these nucleotide regions interact and are in close proximity in the rRNA tertiary structure.[15] The sequences of the *P. multocida* and *E. coli* rRNAs are identical in the region shown; nucleotide modifications are shown for the *E. coli* rRNA; *P. multocida* has the m^5U747 methylation but not m^1G745.[5] Sites of macrolide contact (Table 1) are highlighted in black; tertiary folding of the region is facilitated *via* interaction of A752 with U2609 and C2055 with Ψ2504.

Table 1. Changes in Accessibilities of 23S rRNA Nucleotides upon Macrolide Binding[a]

		intensity changes in chemical modification caused by drug binding at 23S rRNA nucleotides					
source of ribosomes	antibiotics	A752	A2058	A2059	A2062	U2506	U2609
P. multocida 4407	tildipirosin (TIP)	**1.21 ± 0.20**	0.15 ± 0.06	0.23 ± 0.03	**1.47 ± 0.09**	0.90 ± 0.12	0.23 ± 0.05
	tilmicosin (TIL)	0.80 ± 0.07	0.10 ± 0.04	0.22 ± 0.04	**1.35 ± 0.17**	0.90 ± 0.10	0.11 ± 0.04
	tylosin (TYL)	0.73 ± 0.02	0.14 ± 0.01	0.22 ± 0.01	0.25 ± 0.01	0.26 ± 0.04	0.12 ± 0.04
E. coli DH1	tildipirosin (TIP)	**1.22 ± 0.05**	0.14 ± 0.03	0.25 ± 0.07	**1.72 ± 0.09**	0.92 ± 0.07	0.21 ± 0.03
	tilmicosin (TIL)	0.77 ± 0.08	0.15 ± 0.02	0.25 ± 0.02	**1.52 ± 0.14**	0.95 ± 0.11	0.11 ± 0.08
	tylosin (TYL)	0.59 ± 0.05	0.12 ± 0.01	0.19 ± 0.05	0.36 ± 0.02	0.22 ± 0.07	0.14 ± 0.03

[a]Footprinting effects shown here were recorded at 20 μM macrolide concentration (in excess of the K_{diss} values for these drugs). Dropping the drug concentrations to 0.1 μM resulted in minor reductions in the DMS and CMCT protections and enhancements, although the general patterns of chemical reactivity in the rRNA remained unchanged. Values are from at least three independent binding experiments and are compared relative to modified samples without antibiotic, which were set to 1.00 for each nucleotide position studied. Nucleotides showing enhanced accessibility are highlighted in bold. No changes at other nucleotides were observed.

nitrogens, which could not be differentiated. Thus, in free solution at physiological pH, the 23-piperidine would predominantly carry a positive charge. Nevertheless, calculations were made for both the charged and uncharged states of the 23-piperidine nitrogen due to uncertainties about the microenvironment of this group in the ribosome tunnel including, as discussed below, the influence of the nascent peptide chain.

dx.doi.org/10.1021/cb300105p | *ACS Chem. Biol.* 2012, 7, 1351–1355

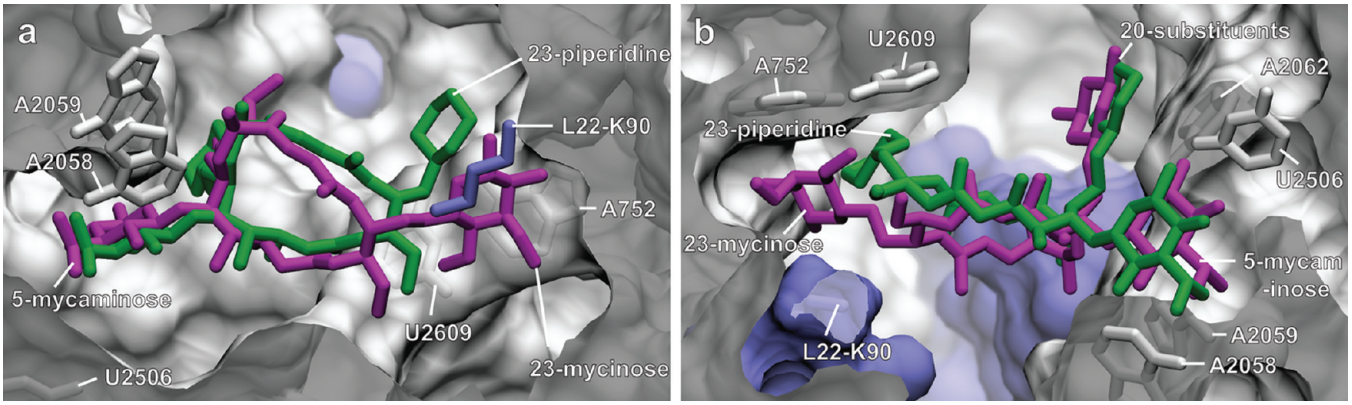

Figure 3. Minimized structures of the 16-membered ring macrolides in their ribosomal binding site. (a) Minimalized structures of TIP (green) and TIL (magenta) superimposed in the ribosomal binding site. Ribosomal residues interacting with the drugs are indicated; nucleotides A752 and U2609 are behind the plane of view. In this view, the site of peptide bond formation at the peptidyl transferase center (PTC) is at the lower left. (b) Alternative viewing angle of the same interactions where the PTC is located at the far right of the panel. When unimpeded by macrolide antibiotics, the peptide chain is initiated at the PTC and then grows through the drug site, passing down the ribosome tunnel following the surface of r-protein L22. In this view, nucleotides A2059 and A2062 are behind the macrolide plane and r-protein L4 is in the background (blue). TIP is shown in the conformation with both piperidines protonated.

Rotation of the protonated 23-piperidine on its linker bonds brings its charged nitrogen into close proximity with nucleotide A752. Minimizing this starting structure, with A752 and the surrounding nucleotides free to move, a new local minimum was identified where the 23-piperidine interacts with A752 *via* the same mechanism as seen with the 20-piperidine and A2062 (Figure 3 and Supplementary Figure 1d). With its nitrogen neutralized, the 23-piperidine would interact further down the tunnel wall with r-protein L22 (Supplementary Figure 1e). Ribosomal protein L22 is known to influence the efficacy of macrolide drugs[20,21] but invariably does so without direct contact within the primary binding site of the drug.[8,9] In both its charged and uncharged conformations, the 23-piperidine of TIP would be positioned further into the lumen of the tunnel relative to the 23-mycinose of TIL and TYL, which interacts with nucleotide G748 in the tunnel wall (Supplementary Figure 5). Methylation at the N1-position of nucleotide G748 causes a steric clash with the 23-mycinose hindering accommodation into the binding site and conferring mild TYL resistance.[12] The same effect is predicted to interfere with binding of TIL, but not for TIP where the 23-piperidine in both its protonated and neutral states would be expected to side-step a direct clash with m^1G748.

rRNA Contacts and Macrolide Mode of Action. The structural models presented here are based on the available empirical data and computational parameters and define the location, orientation, and general conformation of TIP and TIL within their ribosome binding site. The 20- and 23-(dimethyl) piperidines are novel and mechanistically the most intriguingly features of the newer 16-membered macrolides, although they were also difficult substituents to model in the calculated structures. The binding interactions of the piperidines are determined by their protonation state, which in turn is influenced by the immediate environment within the ribosome tunnel. This region of the tunnel is particularly receptive to the sequence of the peptide chain (refs 14 and 22 and references therein), which could feasibly influence the protonation state of the two piperidines of TIP. Comprehensive sampling of a system as large and complicated as the ribosome is presently prohibitive due to computational cost, even without taking an array of nascent peptides into account. It is therefore possible that there are thermodynamically more favorable configurations of the piperidine–adenosine interactions, and it is more than likely that specific drug–peptide contacts remain to be uncovered. We note that the hydrophobic edges of the two piperidines of TIP are angled into the lumen of the tunnel (Figure 3) and compared to TYL (Supplementary Figure 4) could provide an additional barrier to the newly synthesized peptide chain as it attempts to pass through the ribosome.

METHODS

Cell Strains and Growth Conditions. The *P. multocida* field isolate 4407 contains none of the macrolide resistance determinants *erm(42)*, *msr(E)*, and *mph(E)* seen in this species and is consequently sensitive to TIP and other macrolides.[5,6] *E. coli* DH1 is a standard laboratory strain lacking all antibiotic resistance determinants.[23] The *P. multocida* 4407 strain was grown in the absence of antibiotics in 150 mL of brain-heart infusion broth (Oxoid) at 37 °C to an A_{450} of 0.4; *E. coli* DH1 was grown in a similar manner in Lauria-Bertani medium.[23]

Chemical Footprinting of Macrolides on Ribosomes. Ribosomes were prepared from the bacterial strains *P. multocida* 4407 and *E. coli* DH1 as previously described.[18,24] Ribosomes at 10 nM were incubated alone or with 0.1–20 μM concentrations of one of the 16-membered ring macrolides TIP (MSD Animal Health), TIL or TYL (Sigma) in 100 μL of potassium cacodylate buffer and were probed with dimethyl sulfate (DMS) or with 1-cyclohexyl-3-(2-morpholinoethyl)-carbodiimide metho-*p*-toluene sulfonate (CMCT).[17,24] Sites of modification in the rRNA were analyzed with reverse transcriptase (Life Sciences)[24] by extending 5′-[^{32}P]-end-labeled primers hybridized to complementary sequences on the 3′-side of the macrolide binding site around 23S rRNA nucleotides 750, 2058, and 2610 (Supplementary Table 1). Bands on denaturing gels were quantified by phosphorimaging with a GE Healthcare Typhoon 9200 and were normalized for the respective rRNA regions against nucleotides A782, A2082, or U2585, which are situated outside the macrolide binding site and are unaffected by the drugs.

Computational Parameters. Calculations for compounds in free solution and for the model ribosome system were performed in the Schrödinger 2010(U1) Suite. Force fields were calculated with Merck Molecular Force Fields (MMFFs) using the water continuum model with standard settings and charges. Cut-offs of 4.0, 8.0, and 20.0 Å were applied for H-bond, van der Waals, and electrostatic interactions, respectively. Further details about the construction of the model system from the *E. coli* ribosome together with parameters for conformational penalties and quantum mechanical calculations are provided in the Supporting Information.

The pK_a values for the macrolide substituents were determined by a pH-metric (potentiometric) approach under methanol-aqueous

dx.doi.org/10.1021/cb300105p | *ACS Chem. Biol.* 2012, 7, 1351–1355

conditions over a pH range of 3.1 to 10.9 and at sample concentrations between 0.8 and 1.3 mM. Nitrogens shown to be protonated at physiological pH (Figure 1) were taken into account in the calculations.

■ ASSOCIATED CONTENT

Supporting Information

Additional experimental details and figures. Links to PDB files are provided with the calculated coordinates of tylosin (TYL), tilmicosin (TIL), and tildipirosin with two (TIP2) and three protonated nitrogens (TIP3) within the ribosomal binding site. This material is available free of charge *via* the Internet at http://pubs.acs.org.

■ AUTHOR INFORMATION

Corresponding Author

*E-mail: srd@bmb.sdu.dk

Present Address

[§]Dept. of Medical Chemistry, Pharmaceutical Sciences, Universitetsparken 2, 2100 Copenhagen, Denmark.

Notes

The authors declare no competing financial interest.

■ ACKNOWLEDGMENTS

S.D. gratefully acknowledges support from Intervet Innovation GmbH, the Danish Research Agency (FNU-rammebevillinger 09-064292/10-084554), and the Nucleic Acid Center of the Danish Grundforskningsfond. J.P. gratefully acknowledges the Lundbeck Foundation.

■ REFERENCES

(1) Rose, S., Desmolaize, B., Jaju, P., Warrass, R., and Douthwaite, S. (2012) Multiplex PCR to identify macrolide resistance determinants in *Mannheimia haemolytica* and *Pasteurella multocida*. *Antimicrob. Agents Chemother.*, AAC00266−12.

(2) Griffin, D. (2010) Bovine pasteurellosis and other bacterial infections of the respiratory tract. *Vet. Clin. North. Am. Food Anim. Pract. 26*, 57−71.

(3) Katsuda, K., Kohmoto, M., Mikami, O., and Uchida, I. (2009) Antimicrobial resistance and genetic characterization of fluoroquinolone-resistant *Mannheimia haemolytica* isolates from cattle with bovine pneumonia. *Vet. Microbiol. 139*, 74−79.

(4) Michael, G. B., Kadlec, K., Sweeney, M. T., Brzuszkiewicz, E., Liesegang, H., Daniel, R., Murray, R. W., Watts, J. L., and Schwarz, S. (2012) ICEPmu1, an integrative conjugative element (ICE) of *Pasteurella multocida*: analysis of the regions that comprise 12 antimicrobial resistance genes. *J. Antimicrob. Chemother. 67*, 84−90.

(5) Desmolaize, B., Rose, S., Warrass, R., and Douthwaite, S. (2011) A novel Erm monomethyltransferase in antibiotic resistance isolates of *Mannheimia haemolytica* and *Pasteurella multocida*. *Mol. Microbiol. 80*, 184−194.

(6) Desmolaize, B., Rose, S., Wilhelm, C., Warrass, R., and Douthwaite, S. (2011) Combinations of macrolide resistance determinants in field isolates of *Mannheimia haemolytica* and *Pasteurella multocida*. *Antimicrob. Agents Chemother. 55*, 4128−4133.

(7) Kadlec, K., Brenner Michael, G., Sweeney, M. T., Brzuszkiewicz, E., Liesegang, H., Daniel, R., Watts, J. L., and Schwarz, S. (2011) Molecular basis of macrolide, triamilide, and lincosamide resistance in *Pasteurella multocida* from bovine respiratory disease. *Antimicrob. Agents Chemother. 55*, 2475−2477.

(8) Hansen, J. L., Ippolito, J. A., Ban, N., Nissen, P., Moore, P. B., and Steitz, T. A. (2002) The structures of four macrolide antibiotics bound to the large ribosomal subunit. *Mol. Cell 10*, 117−128.

(9) Wilson, D. N., Harms, J. M., Nierhaus, K. H., Schlunzen, F., and Fucini, P. (2005) Species-specific antibiotic-ribosome interactions: implications for drug development. *Biol. Chem. 386*, 1239−1252.

(10) Poulsen, S. M., Kofoed, C., and Vester, B. (2000) Inhibition of the ribosomal peptidyl transferase reaction by the mycarose moiety of the antibiotics carbomycin, spiramycin and tylosin. *J. Mol. Biol. 304*, 471−481.

(11) Petropoulos, A. D., Kouvela, E. C., Dinos, G. P., and Kalpaxis, D. L. (2008) Stepwise binding of tylosin and erythromycin to *Escherichia coli* ribosomes, characterized by kinetic and footprinting analysis. *J. Biol. Chem. 283*, 4756−4765.

(12) Liu, M., and Douthwaite, S. (2002) Resistance to the macrolide antibiotic tylosin is conferred by single methylations at 23S rRNA nucleotides G748 and A2058 acting in synergy. *Proc. Natl. Acad. Sci. U.S.A. 99*, 14658−14663.

(13) Poehlsgaard, J., and Douthwaite, S. (2005) The bacterial ribosome as a target for antibiotics. *Nat. Rev. Microbiol. 3*, 870−881.

(14) Starosta, A. L., Karpenko, V. V., Shishkina, A. V., Mikolajka, A., Sumbatyan, N. V., Schluenzen, F., Korshunova, G. A., Bogdanov, A. A., and Wilson, D. N. (2010) Interplay between the ribosomal tunnel, nascent chain, and macrolides influences drug inhibition. *Chem. Biol. 17*, 504−514.

(15) Dunkle, J. A., Xiong, L., Mankin, A. S., and Cate, J. H. (2010) Structures of the *Escherichia coli* ribosome with antibiotics bound near the peptidyl transferase center explain spectra of drug action. *Proc. Natl. Acad. Sci. U.S.A. 107*, 17152−17157.

(16) Vazquez-Laslop, N., Thum, C., and Mankin, A. S. (2008) Molecular mechanism of drug-dependent ribosome stalling. *Mol. Cell 30*, 190−202.

(17) Moazed, D., and Noller, H. F. (1987) Chloramphenicol, erythromycin, carbomycin and vernamycin B protect overlapping sites in the peptidyl transferase region of 23S ribosomal RNA. *Biochimie 69*, 879−884.

(18) Hansen, L. H., Mauvais, P., and Douthwaite, S. (1999) The macrolide-ketolide antibiotic binding site is formed by structures in domains II and V of 23S ribosomal RNA. *Mol. Microbiol. 31*, 623−632.

(19) Xiong, L., Shah, S., Mauvais, P., and Mankin, A. S. (1999) A ketolide resistance mutation in domain II of 23S rRNA reveals the proximity of hairpin 35 to the peptidyl transferase centre. *Mol. Microbiol. 31*, 633−639.

(20) Chittum, H. S., and Champney, W. S. (1994) Ribosomal protein gene sequence changes in erythromycin-resistant mutants of *Escherichia coli*. *J. Bacteriol. 176*, 6192−6198.

(21) Lawrence, M. G., Lindahl, L., and Zengel, J. M. (2008) Effects on translation pausing of alterations in protein and RNA components of the ribosome exit tunnel. *J. Bacteriol. 190*, 5862−5869.

(22) Vazquez-Laslop, N., Ramu, H., Klepacki, D., Kannan, K., and Mankin, A. S. (2011) The key function of a conserved and modified rRNA residue in the ribosomal response to the nascent peptide. *EMBO J. 29*, 3108−3117.

(23) Sambrook, J., and Russell, D. W. (2001) *Molecular Cloning: A Laboratory Manual*, 3rd ed., Cold Spring Harbor Press, Cold Spring Harbor.

(24) Stern, S., Moazed, D., and Noller, H. F. (1988) Structural analysis of RNA using chemical and enzymatic probing monitored by primer extension. *Methods Enzymol. 164*, 481−489.